JCI The Journal of Clinical Investigation

Real-time imaging of trapping and urease-dependent transmigration of *Cryptococcus neoformans* in mouse brain

Meiqing Shi, … , Paul Kubes, Christopher H. Mody

J Clin Invest. 2010;120(5):1683-1693. https://doi.org/10.1172/JCI41963.

Research Article

Infectious meningitis and encephalitis is caused by invasion of circulating pathogens into the brain. It is unknown how the circulating pathogens dynamically interact with brain endothelium under shear stress, leading to invasion into the brain. Here, using intravital microscopy, we have shown that *Cryptococcus neoformans*, a yeast pathogen that causes meningoencephalitis, stops suddenly in mouse brain capillaries of a similar or smaller diameter than the organism, in the same manner and with the same kinetics as polystyrene microspheres, without rolling and tethering to the endothelial surface. Trapping of the yeast pathogen in the mouse brain was not affected by viability or known virulence factors. After stopping in the brain, *C. neoformans* was seen to cross the capillary wall in real time. In contrast to trapping, viability, but not replication, was essential for the organism to cross the brain microvasculature. Using a knockout strain of *C. neoformans*, we demonstrated that transmigration into the mouse brain is urease dependent. To determine whether this could be amenable to therapy, we used the urease inhibitor flurofamide. Flurofamide ameliorated infection of the mouse brain by reducing transmigration into the brain. Together, these results suggest that *C. neoformans* is mechanically trapped in the brain capillary, which may not be amenable to pharmacotherapy, but actively transmigrates to the brain parenchyma with contributions from urease, suggesting that a […]

Real-time imaging of trapping and urease-dependent transmigration of *Cryptococcus neoformans* in mouse brain

Meiqing Shi,[1] Shu Shun Li,[1] Chunfu Zheng,[2] Gareth J. Jones,[1] Kwang Sik Kim,[3] Hong Zhou,[4] Paul Kubes,[4] and Christopher H. Mody[1,5]

[1]Department of Microbiology and Infectious Diseases, University of Calgary, Calgary, Alberta, Canada. [2]State Key Laboratory of Virology, Wuhan Institute of Virology, Chinese Academy of Sciences, Wuhan, China. [3]Division of Pediatric Infectious Diseases, Johns Hopkins University School of Medicine, Baltimore, Maryland, USA. [4]Department of Physiology and Biophysics and [5]Department of Internal Medicine, University of Calgary, Calgary, Alberta, Canada.

Infectious meningitis and encephalitis is caused by invasion of circulating pathogens into the brain. It is unknown how the circulating pathogens dynamically interact with brain endothelium under shear stress, leading to invasion into the brain. Here, using intravital microscopy, we have shown that *Cryptococcus neoformans*, a yeast pathogen that causes meningoencephalitis, stops suddenly in mouse brain capillaries of a similar or smaller diameter than the organism, in the same manner and with the same kinetics as polystyrene microspheres, without rolling and tethering to the endothelial surface. Trapping of the yeast pathogen in the mouse brain was not affected by viability or known virulence factors. After stopping in the brain, *C. neoformans* was seen to cross the capillary wall in real time. In contrast to trapping, viability, but not replication, was essential for the organism to cross the brain microvasculature. Using a knockout strain of *C. neoformans*, we demonstrated that transmigration into the mouse brain is urease dependent. To determine whether this could be amenable to therapy, we used the urease inhibitor flurofamide. Flurofamide ameliorated infection of the mouse brain by reducing transmigration into the brain. Together, these results suggest that *C. neoformans* is mechanically trapped in the brain capillary, which may not be amenable to pharmacotherapy, but actively transmigrates to the brain parenchyma with contributions from urease, suggesting that a therapeutic strategy aimed at inhibiting this enzyme could help prevent meningitis and encephalitis caused by *C. neoformans* infection.

Introduction

Infectious meningitis and encephalitis is a devastating disease associated with high mortality and morbidity throughout the world. For disease to develop, the circulating pathogen must be arrested in the brain vasculature and then cross the blood vessels of the leptomeninges or pia mater and gain access to the brain and meninges (1, 2). Unfortunately, little is known about how this occurs for many microorganisms. In this study, using novel in vivo spinning disk imaging, we examined how *Cryptococcus neoformans*, a pathogen causing human and animal meningoencephalitis, interacts dynamically with the brain endothelium in the murine host, leading to the penetration of the brain microvasculature.

C. neoformans is an encapsulated budding yeast that causes fatal infections, especially in immunocompromised individuals, including patients with HIV infection (3). After the aerosolized fungal cells are inhaled, they multiply in the lung, resulting in infection (4, 5). From there, extrapulmonary dissemination occurs, leading to infection of the bloodstream and subsequent hematogenous dissemination to target organs (3, 6). After this, the infectious particle must be arrested in the infected tissue. In the case of an organism such as *C. neoformans*, the process that brings the organisms to arrest could be a mechanical process (trapping, such as septic emboli) or a biological process (receptor-mediated adhesion, such as leukocyte or *Borrelia burgdorferi* adhesion; refs. 7 and 8). It follows that tissue invasion could be a mechanical process (previously suggested to be due to proliferation of the organism, expansion of the colony with subsequent bursting of the vasculature and penetration into the brain) or a biologic process (e.g., receptor-mediated invasion by *Escherichia coli* K1 and *Streptococcus pneumoniae*; refs. 9, 10). This is more than just a trivial issue, since therapeutic approaches would be quite disparate depending on the mechanism involved.

Unfortunately, due to prior limitations in experimental approaches, there have been no studies directly addressing the question of how *C. neoformans* stops in the brain microvasculature before crossing. Nor is it completely understood how crossing occurs, despite much effort (6, 11–16). In vitro experiments demonstrated that *C. neoformans* is internalized by human umbilical vein endothelial cells (HUVECs) (14) or human brain microvascular endothelial cells (HBMECs) (11). In those model systems, *C. neoformans* is stationary and in prolonged contact with the surface of endothelial cells. However, in vivo, *C. neoformans* is circulating in the blood under flow conditions, driven by vascular pressure, and therefore models using stationary cells are potentially misleading. Histology has shown that *C. neoformans* is located in intimate association with the endothelium and in the parenchyma outside of blood vessels in the brain after infection (12, 15). Although this implies a process whereby *C. neoformans* crosses the brain microvasculature, these events have not been observed in vivo.

In this study, we established a real-time experimental model system in which we used a variety of intravital microscopy (IVM) techniques to directly visualize the early dynamic interaction of *C. neoformans* with the brain microvasculature in mice. These techniques permit spatial and kinetic resolution of the endothelial interac-

Conflict of interest: The authors have declared that no conflict of interest exists.
Citation for this article: *J Clin Invest.* 2010;120(5):1683–1693. doi:10.1172/JCI41963.

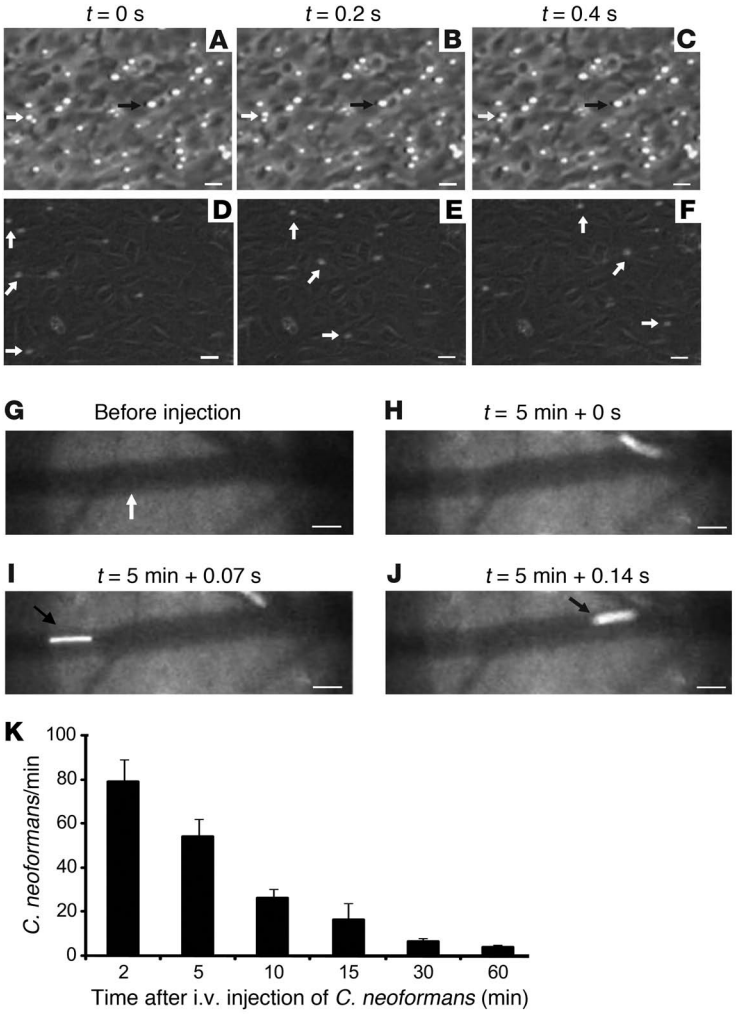

Figure 1

C. neoformans does not roll and adhere to endothelial cells under flow conditions in vitro or to postcapillary venules in vivo. Monolayers of HUVECs on glass coverslips were treated with 10 ng/ml LPS. Leukocytes or *C. neoformans* (10^6/ml) were perfused over the monolayers of the endothelial cells at 2 dyn/cm^2. (**A**–**C**) A series of images taken by phase contrast microscopy showing the rolling leukocytes (white arrows) and stationary leukocytes (black arrows). (**D**–**F**) A series of images taken by phase contrast microscopy, with the imaging optimized to show the movement of the yeast cells (white arrows). Time in seconds is shown. Mice were anesthetized, and the brain microcirculation was visualized by IVM. *C. neoformans* (100×10^6 strain H99) labeled with FITC were suspended in 100 μl saline and injected via the tail vein. (**G**) An image of a postcapillary venule (white arrow) before injection of *C. neoformans*. (**H**–**J**) A series of images of the same capillary taken 5 minutes after injection; time in minutes and seconds. Black arrows indicate the same moving yeast cell. Scale bars: 20 μm. (**K**) Numbers of *C. neoformans* passing a fixed point in a postcapillary venule (with a diameter between 30 and 70 μm) at various times after injection. Data are expressed as mean ± SEM of 2 independent experiments (n = 8 mice).

tion with the yeast cells in real time. We also sought to capture direct evidence for the crossing of the brain microvasculature by *C. neoformans* in vivo using immunofluorescence microscopy and to visualize the yeast crossing the brain microvasculature in animals using spinning disk confocal IVM. Finally, we assessed factors that have the potential to affect the subsequent invasion of the brain microvasculature in vivo using mutant strains of *C. neoformans* and pharmacologic inhibition.

Results

Unlike leukocytes, C. neoformans does not roll and adhere to endothelial cells under flow conditions in vitro or to postcapillary venules in vivo. To examine the interaction of *C. neoformans* with the endothelium, we initially performed experiments in a system where the microorganism was moving across the endothelial cells without the confounding influences of a vascular structure of varying diameter and branches, and in which we could precisely control the shear stress. For this purpose, we used an in vitro flow chamber to observe the interaction of *C. neoformans* with a monolayer of endothelial cells (HUVECs). This allowed us to determine whether there was a reduction in velocity, followed by arrest on the endothelium, much the same way that leukocytes roll and stop on the endothelium (17, 18). If this were to occur, organisms interacting with the endothelial surface would be moving with a reduced velocity compared with those organisms that were not interacting. As a positive control, the movement of human leukocytes was examined. In these experiments, leukocytes that were moving at the same velocity as the buffer moved across the field of view so quickly that they could not be seen. Some leukocytes moved only a short distance over 0.4 seconds (white arrows, Figure 1, A–C, and Supplemental Video 1; supplemental material available online with this article; doi:10.1172/JCI41963DS1), indicating that they were moving more slowly than the buffer, consistent with rolling. Moreover, other leukocytes remained in the same position, indicating they were adherent to the endothelial cells (black arrows, Figure 1, A–C, and Supplemental Video 1). Thus, leukocytes roll and adhere to an LPS-activated HUVEC monolayer at a shear of 2 dyn/cm^2, which is typical of the shear forces in vivo. By contrast, *C. neoformans* moved across the entire field in 0.4 seconds, which was the same velocity as the buffer (white arrows, Figure 1, D–F, and Supplemental Video 2). Further, the movement of *C. neoformans* across HUVECs that had been pretreated with LPS was not different from movement across endothelium that had not been pretreated (data not shown). Reasoning that the interaction might be relatively weak, we reduced the velocity to produce shear of 1, 0.5, 0.25, 0.13, 0.06, or 0.03 dyn/cm^2. Even at these low shears, which are lower than in any vascular bed, we were still unable to observe any evidence of rolling and adhesion (data not shown). Additionally, we were

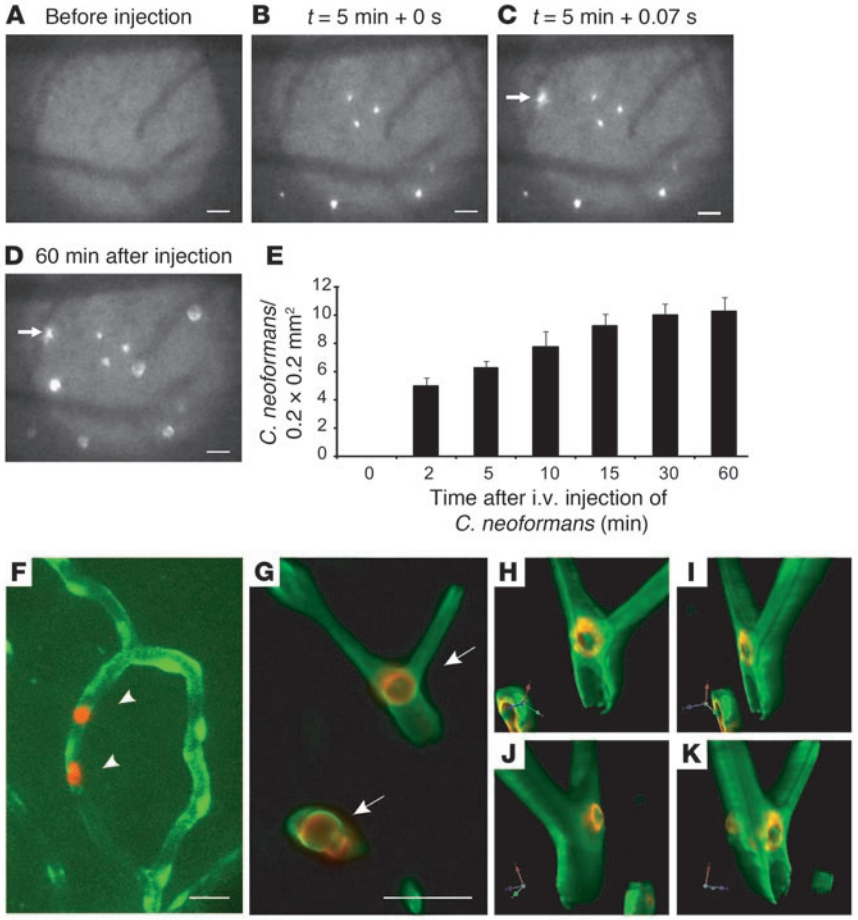

Figure 2
C. neoformans stops suddenly in the brain capillaries. *C. neoformans* (strain H99) labeled with FITC was injected via the tail vein. (**A**) An image of the brain capillary bed before injection of *C. neoformans*. (**B** and **C**) Images taken by IVM showing the same field of view 5 minutes after injection. Time in minutes and seconds is shown. (**D**) An image was taken by IVM showing the same field of view 60 minutes after injection. Arrows indicate the same yeast immediately following arrest and when stationary. (**E**) The number of stationary *C. neoformans* in a field of view at various time points after injection. Data are expressed as mean ± SEM of 2 independent experiments (n = 8 mice). (**F**) Tie-2 GFP mice (which allowed visualization of the capillaries in vivo) were anesthetized, and spinning disk confocal microscopy of the brain microcirculation was performed. *C. neoformans* (100×10^6 strain H99) labeled with TRITC (arrowhead) in 100 μl saline was injected via tail vein. (**G**) Mice were injected with 20×10^6 *C. neoformans* (strain H99) via the tail vein. Sixty minutes later, the mice were anesthetized, and vascular perfusion was performed. The brain was removed, and immunohistochemistry was performed using anticryptococcal antibody (red, arrows) and anti–collagen IV (green). The images in **H**–**K** are 3D reconstructive images of the image in **G**. Scale bars: 20 μm.

also unable to see any evidence of rolling or adhesion on a cell line of HBMECs (Supplemental Video 3). Moreover, we did not see yeast crossing the endothelial cells under flow conditions. Thus, there was no evidence of an interaction of *C. neoformans* with an endothelial monolayer under shear conditions in vitro.

The above observation that *C. neoformans* did not roll and adhere to endothelial cells under flow conditions in vitro raised a question about the process by which *C. neoformans* would stop in the brain in vivo. To address this question, we established IVM of the brain microvasculature to visualize the yeast cells and brain vasculature in the murine host in real time. This technique allowed us to visualize the pial and superficial cortical vasculature (19, 20), which is adjacent to the meninges. *C. neoformans* appeared in the brain microvasculature within 3.4 ± 0.4 seconds (n = 8 mice) after injection into the tail vein, indicating a surprisingly rapid transit through the lung following i.v. inoculation.

The brain postcapillary vessels are replete with vascular adhesion molecules allowing for the dynamics of leukocyte transmigration (21, 22). Thus, we first investigated whether *C. neoformans* roll and adhere in the postcapillary venule, behaving similarly to leukocytes during inflammation. In a sequence of images, spherical organisms were moving so fast that they were seen as luminescent streaks in images separated by 0.07 seconds, appearing to move with the same velocity as the blood, and there were no organisms that were arrested in the postcapillary venule (Figure 1, G–J, and Supplemental Video 4). The number of yeast cells passing through postcapillaries was greatest immediately after injection and gradually decreased over time, such that at 60 minutes, only a small number of organisms could be seen passing through the vasculature (Figure 1K). However, even after 18 hours, rare organisms could still be seen moving in the vascular compartment of the brain (data not shown). To determine whether prior inflammation alters the interaction of *C. neoformans* in the brain, we treated mice with LPS and then injected *C. neoformans* 4 hours later. There was no change in the transit of *C. neoformans* through the postcapillary venule after pretreatment with LPS (data not shown).

C. neoformans stops suddenly in the brain capillary. Strikingly, the yeast cells appeared to move at the same speed as the blood flow and came to a sudden stop in the capillary bed (Figure 2, A–D, and Supplemental Video 5). No fluorescence was seen before injection (Figure 2A). The yeast stopped suddenly in the capillary bed as soon as 23.0 ± 3.7 seconds (n = 8 mice) after i.v. injection, and there was no evidence of a reduction in velocity prior to stopping within the vasculature that would be consistent with rolling. In a series of images taken 5 minutes after injection, some organisms had stopped (Figure 2B). In the next image (0.07 seconds later), an organism suddenly appeared that was not present in the prior frame (Figure 2C, arrow). This organism remained stationary for the whole period of observation (60 minutes after injection) (Figure 2D, arrow). There was a steady increase in the number of organisms over the 60-minute observation period, such that more yeast cells were seen in the same capillary bed (Figure 2D). The

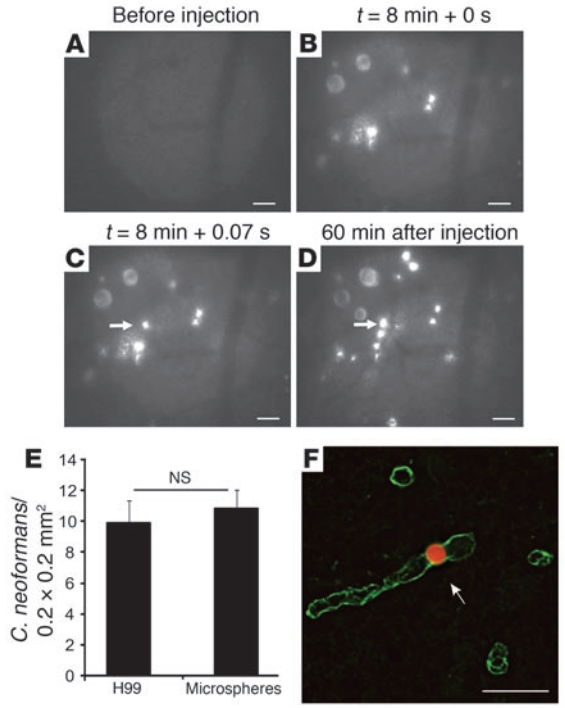

Figure 3
Polystyrene microspheres stop in the brain with the same kinetics as *C. neoformans*. Fluorescent polystyrene microspheres that are similar in size to *C. neoformans* (strain H99) in 100 μl saline were injected via tail vein. (**A**) An image of the brain capillary bed before injection of microspheres. (**B** and **C**) A series of images taken by IVM showing the same field of view 8 minutes after injection. The arrow indicates a suddenly arrested microsphere. (**D**) An image was taken by IVM showing the same field of view 60 minutes after injection. The arrow indicates the same microsphere after suddenly trapping shown in **C**. Time in minutes and seconds is shown. (**E**) Numbers of stationary *C. neoformans* in the capillary bed 60 minutes after injection of microspheres or *C. neoformans* (H99). Data are expressed as mean ± SEM of 2 independent experiments ($n = 8$). (**F**) C57BL/6 mice were injected with 20×10^6 microspheres (red, arrow) via the tail vein. Sixty minutes later, the mice were anesthetized and perfusion was performed. The brain was removed for frozen sections as described in Methods. Immunohistochemistry was performed to label vessels (green). Scale bars: 20 μm.

majority of *C. neoformans* that came to a stop did so within the first few minutes, while progressively fewer organisms were arrested over the period of observation (Figure 2E). The kinetics and location of arrest were similar using CFSE-labeled *C. neoformans* (data not shown), suggesting that the method of labeling did not impact the kinetics of transit and arrest of *C. neoformans*.

Using spinning disk confocal microscopy and immunohistochemistry, the stationary organisms were shown to be detained in capillaries that appeared to be of the same diameter as the organism, often at branch points (Figure 2, F and G, and Figure 2, H–K, which is a rotational 3D reconstruction of Figure 2G). By analyzing successive frames before each organism came to a halt, we were able to determine that 70% ± 3% of the organisms originated from penetrating vessels deep within the brain, while the remainder were arrested while traveling in pial surface vessels. Moreover, there was a linear relationship between the number of organisms injected and the number that stopped. The total number of yeasts in 20 microscopic fields was 8.7 ± 1.9, 78.0 ± 16.3, and 808.3 ± 111.9 ($n = 6$ mice) after injection of 1×10^6, 10×10^6, and 100×10^6 yeasts, respectively. Thus, our data demonstrate that *C. neoformans* was suddenly arrested in the brain capillary, in locations of vessel narrowing without slowing before stopping, and the number of organisms stopping was linearly related to the number injected.

Differences in viability, polysaccharide capsule, and strain fail to affect deposition in the brain, which is similar to that of inert particles. We reasoned that altering virulence or viability of the organisms would influence potential receptor-ligand interactions, leading to arrest. To test this hypothesis, we compared wild-type organisms with organisms that were killed by heating, organisms with no polysaccharide capsule (the major virulence factor), or *C. neoformans var. grubii*, which has a greater prevalence and therefore presumed virulence than *C. neoformans var. neoformans* (23). Mice were injected with fluorochrome-labeled live strain H99 (*C. neoformans var. grubii*), heat-killed H99, B3501 (*C. neoformans var. neoformans*), or Cap67 (an acapsular mutant of strain B3501). In some experiments, 2 organisms were compared by simultaneous injection of equal numbers of 2 strains labeled with 2 different fluorochromes. There was no difference in the kinetics of trapping of the yeast in the brain (data not shown and Supplemental Video 6).

The observation that viability and encapsulation did not affect the ability of *C. neoformans* to stop in the brain made us question whether the dynamic process was independent of the organism and whether an inert particle of the same size might behave similarly. To examine this question, we injected mice with polystyrene microspheres that were of similar size to *C. neoformans*. We found that size-matched polystyrene microspheres appeared in the brain microvasculature very shortly after i.v. injection (4.0 ± 0.6 seconds, $n = 8$ mice), which was similar to the time that it took for *C. neoformans* to appear in the brain. Remarkably, polystyrene microspheres could be seen to stop suddenly in the capillary bed as soon as 25 ± 0.5 seconds ($n = 8$ mice) after i.v. injection, which was similar to the time following injection of *C. neoformans*. The number of polystyrene microspheres trapping in the capillary bed increased with time (Figure 3, A–D, and Supplemental Video 7). In a series of figures of the brain capillary bed, no microspheres were seen before injection (Figure 3A). A considerable number of fluorescent microspheres were trapped in the capillary bed 8 minutes after injection (Figure 3B). In the next image (0.07 seconds later), a microsphere appeared that was not seen in the prior frame (Figure 3C, arrow), indicating that the microsphere had suddenly stopped and remained stationary for the duration of observation (Figure 3, C and D, arrows). Indeed, the number of polystyrene microspheres stopping in the capillary bed was similar to the number of *C. neoformans* stationary within the brain 60 minutes after i.v. injection (Figure 3E). Fluorescence microscopy confirmed that polystyrene microspheres were located inside the capillary (Figure 3F). Thus, there was no significant difference in the arrest of polystyrene microspheres in brain capillary bed when compared with *C. neoformans*. Additionally, an avirulent yeast, *Saccharomyces cerevisiae*, was also arrested in the brain similarly to polystyrene beads (Supplemental Video 8), and *C. neoformans* was stopped in other vascular beds (Supplemental Video 9). This is most consistent with mechanical trapping.

Real-time visualization of the crossing of C. neoformans at the capillary level in living mice. The preceding results indicate that the yeast stops suddenly in the brain capillaries, raising the question of whether the stationary yeast cells cross the brain microvasculature

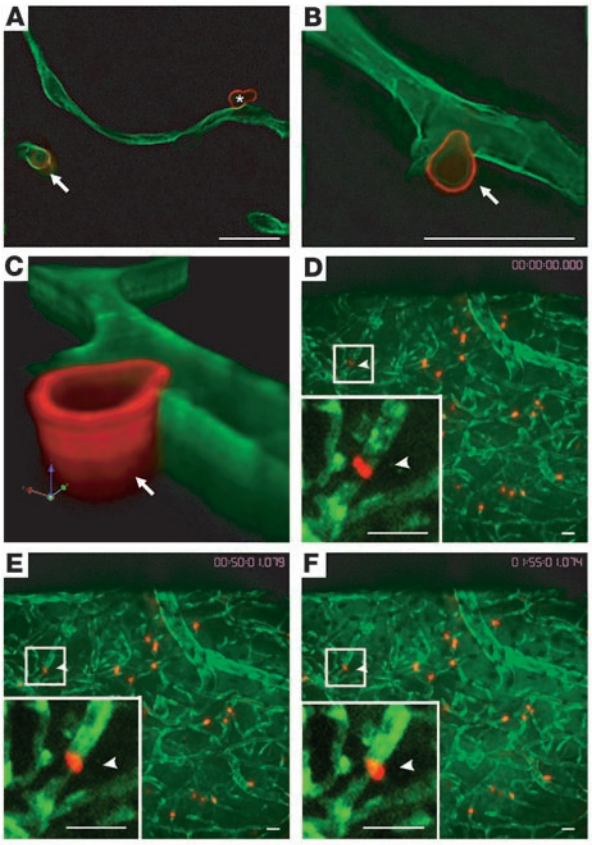

Figure 4
Real-time visualization of *C. neoformans* transmigration in the capillary of a living host. Mice were injected with 20 × 10^6 *C. neoformans* (strain H99) via the tail vein. Six hours later, the brain was removed, and immunohistochemistry was performed to label *C. neoformans* (red) and vessels (green). (**A**) *C. neoformans* was found partially within (arrow) or outside (asterisk) the vessels. (**B** and **C**) Relationship between *C. neoformans* (arrow) and the vessel. (**C**) 3D reconstructive image of **B**. (**D**–**F**) *C. neoformans* (arrowhead) crossing the capillary wall in a living host. Tie-2 GFP BALB/c mice were injected with 100 × 10^6 H99 via the tail vein. The mice were anesthetized, and spinning disk confocal microscopy of the brain microcirculation was performed as described in Methods. Time-lapse video was taken 3 hours after injection of *C. neoformans*. A series of single *z*-stack images is shown. (**D**) At the start of image acquisition, *C. neoformans* was present within the capillaries (arrowhead). *C. neoformans* (arrowheads) moving out from the capillaries across the vessel wall at 50 minutes (**E**) and 1 hour and 55 minutes (**F**). Squares represent areas enlarged in insets. Scale bars: 20 μm.

from this location. Direct evidence showing crossing of the brain microvasculature in vivo has not previously been demonstrated, although *C. neoformans* was shown by histology to be present in the parenchyma outside of blood vessels after infection (12, 15). Thus, we sought to capture images of this process. *C. neoformans* was found outside the brain capillary 6 hours after i.v. injection (asterisk, Figure 4A), indicating that some of the yeast had completed crossing of the capillary at that time. *C. neoformans* could be seen in the process of crossing the capillary wall, with part of the organism outside the capillary and part still inside the capillary (Figure 4, B and C [a 3D reconstruction of the same image], and Supplemental Video 10). This result encouraged us to visualize the crossing of brain microvasculature by *C. neoformans* in real time in living mice. Using spinning disk confocal IVM, we were able to capture a series of images illustrating the dynamic process of the crossing of capillaries by *C. neoformans* in the live animal (Figure 4, D–F). Thus, we provide direct in vivo evidence that *C. neoformans* crosses the brain capillary following a sudden arrest.

Viability is required for transmigration from the capillaries into the brain. We were struck by the observation that *C. neoformans* often displayed an ovoid, budded morphology during transmigration. This was reminiscent of the morphologic change filamentous fungi undergo when invading plants via turgor pressure (24). Since this would require the organism to be viable, experiments were performed to compare transmigration of live versus killed organisms. We found that 11.6% ± 1.8% of live yeast cells were located in the brain parenchyma 24 hours after injection (Figure 5, A and D). By contrast, no heat-killed yeast cells were detected outside the capillary at 24 hours (Figure 5, B and D) or 72 hours after injection (data not shown), suggesting that *C. neoformans* must be viable to cross the capillary. Further, polystyrene microspheres were lodged inside the capillary (Figure 5C) at 24 and 72 hours but were never observed to transmigrate (Figure 5D), further supporting that transmigration is an active process and that viability is essential.

Transmigration from the capillaries to the brain is independent of proliferation. Once *C. neoformans* is trapped in the brain capillary, the yeast transmigrates to the parenchyma. While this might happen directly, Olszewski et al. have suggested that the process might also involve proliferation in the microvasculature and that through the process of proliferation, the colony would expand, rupture, and thereby penetrate the endothelium (15). To examine whether transmigration of *C. neoformans* from capillaries to parenchyma is dependent on fungal proliferation within the vessels, we injected mice via the i.v. route with one of two different temperature-sensitive strains. The *C. neoformans ras1* mutant (25) and the *cdc24* mutant (26) possess a temperature-dependent defect in actin polarization that prevents them from undergoing proper and efficient budding and proliferation. The strains had a greater than 99% inhibition of growth at 37°C compared with 30°C. As a control, we injected mice with the respective reconstituted strains. As expected, the reconstituted strains *ras1* + *RAS1* (Figure 6, A and C) and *cdc24* + *CDC24* (Figure 6, D and F) were detected in the parenchyma of the brain 24 hours after i.v. injection. Remarkably, the same percentages of the temperature-sensitive strains *ras1* (10.8% ± 1.3% versus 11.3% ± 1.9%; Figure 6, B and C) and *cdc24* (11.6% ± 1.8% versus 12.5% ± 1.0%; Figure 6, E and F) were found in the parenchyma of the brain as compared with the reconstituted strains. Therefore, the transmigration of *C. neoformans* from the capillaries to the brain is independent of proliferation of the yeast.

Transmigration of C. neoformans in the brain is urease dependent. Although proliferation is not required for the transmigration, viability is essential. We reasoned that a metabolic process would be required, rather than a receptor that might be displayed regardless of viability. Urease was recently identified as an important virulence factor of *C. neoformans* (15, 27). Thus, we examined the contribution of urease to transmigration in the brain. First, we found that mice survived significantly longer when injected with the urease-knockout strain *ure1* as compared with the wild-type strain H99 or urease-restored strain *ure1*+*URE1*-1 (Figure 7A, $P < 0.01$). Next we assessed the number of CFUs in the brain of mice after infection. Mice infected

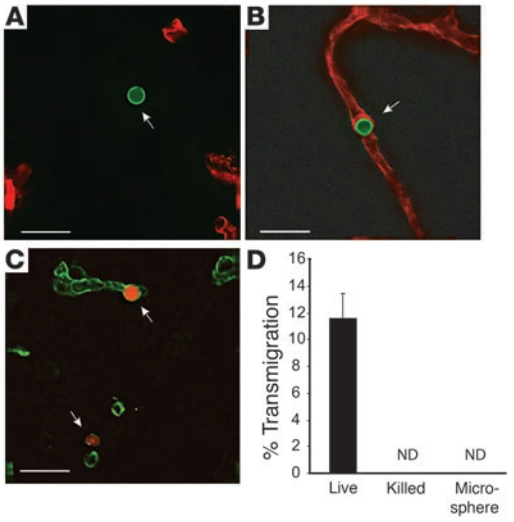

Figure 5
Viability is required for *C. neoformans* transmigration in the brain. Mice were injected with 20 × 10^6 FITC-labeled live strain H99 (**A**, vessel appears red; *C. neoformans* appears green [arrow]), heat-killed strain H99 (**B**, vessel, red; *C. neoformans*, green [arrow]), fluorescence-labeled polystyrene microspheres (**C**; vessel, green; microspheres, red [arrows]). Twenty-four hours later, the mice were anesthetized, and perfusion was performed. The brain was removed, and immunohistochemistry was performed. Scale bars: 20 μm. (**D**) The percentage of the yeasts and polystyrene microspheres located in parenchyma of the brain. Data are presented as mean ± SEM (n = 5). Data are representative of 2 independent experiments. ND, none detected.

with strain H99 or the reconstituted strain *ure1+URE1*-1 had significantly higher CFU counts in the brain at 72 hours after infection as compared with strain *ure1* (Figure 7B, $P < 0.01$). Experiments were then performed to determine whether urease promotes trapping, transmigration, or replication of *C. neoformans* in the brain. There was no significant difference in CFU counts in the brain among the 3 strains shortly after injection (3 hours, Figure 7B), suggesting that urease does not affect the yeast trapping in the brain. To provide additional evidence, the same mice were injected with equal numbers (50 × 10^6) of *ure1* and *ure1+URE1*-1 *C. neoformans* that had been labeled with 2 different fluorochromes, which allowed us to examine the kinetics of both yeasts within the same experiment using spinning disk confocal microscopy. The time to first appearance and transit through the brain was similar (data not shown), and the numbers of yeasts trapped in the capillary at 2 hours after infection were not significantly different (156 ± 28/mm^2 for *ure1* versus 175 ± 25/mm^2 for *ure1+URE1*-1; Figure 7C), indicating that urease does not affect the trapping of the yeast in the brain.

We considered two possibilities to explain the increased CFU counts and mortality. Urease might increase the number of transmigration sites with the same rate of replication at each site, or it might not influence the number of transmigration sites but might permit increased growth of the organism at each site. Immunohistochemistry was performed to enumerate the numbers of organism in each colony and to determine the number of colonies (transmigration sites) in the brain 72 hours after infection. These studies revealed that there was no significant difference in the numbers of organisms at each transmigration site (Figure 7D), suggesting that urease does not enhance the replication of *C. neoformans* in the brain. However, we found that the yeasts were still localized inside the vessels at 24 hours after infection of *ure1* and were rarely seen in the parenchyma (Figure 7E). By contrast, a considerable number of organisms were localized in the parenchyma at 24 hours after injection of *ure1+URE1*-1 (Figure 7F) or wild-type H99 (data not shown). Quantitation revealed that there were 3-fold fewer transmigration sites after injection of *ure1* as compared with wild-type H99 and

Figure 6
Transmigration of temperature-sensitive strains of *C. neoformans* from capillaries to the brain. Mice were injected with 10 × 10^6 FITC-labeled *C. neoformans* strains *ras1* mutant, *cdc24* mutant, reconstituted *ras1* + *RAS1*, or reconstituted *cdc24* + *CDC24* via the tail vein. Twenty-four hours later, the mice were anesthetized, perfusion was performed, and immunohistochemistry was performed. (**A**) Injection of *ras1* + *RAS1* reconstituted strain. (**B**) Injection of *ras1* mutant strain. (**C**) The percentage of the yeasts in the parenchyma. Data are expressed as mean ± SEM of 2 independent experiments (n = 6). (**D**) Injection of *cdc24* + *CDC24* reconstituted strain. (**E**) Injection of *cdc24* mutant strain *C. neoformans*. (**F**) The percentage of the yeasts in the parenchyma. Data are expressed as mean ± SEM of 2 independent experiments (n = 6). *C. neoformans* (arrows), green; vessels, red. Scale bars: 20 μm.

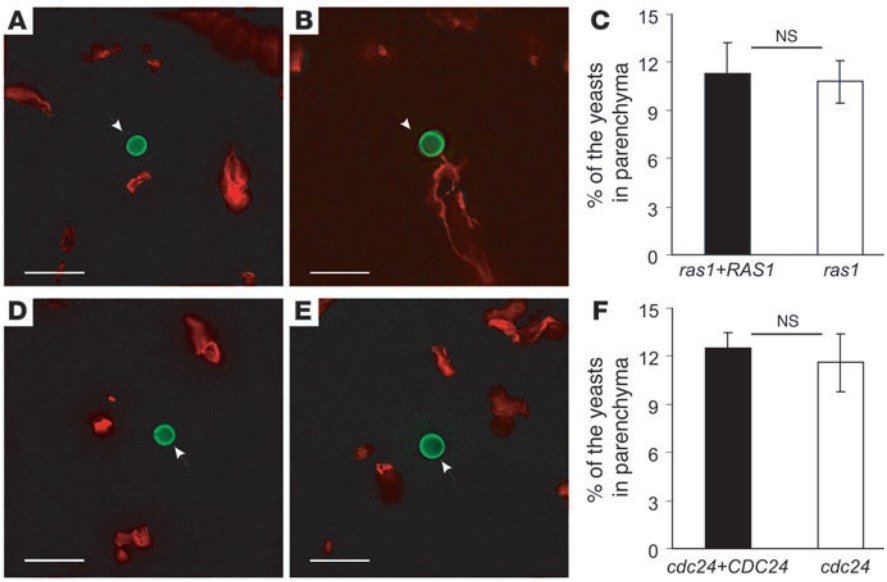

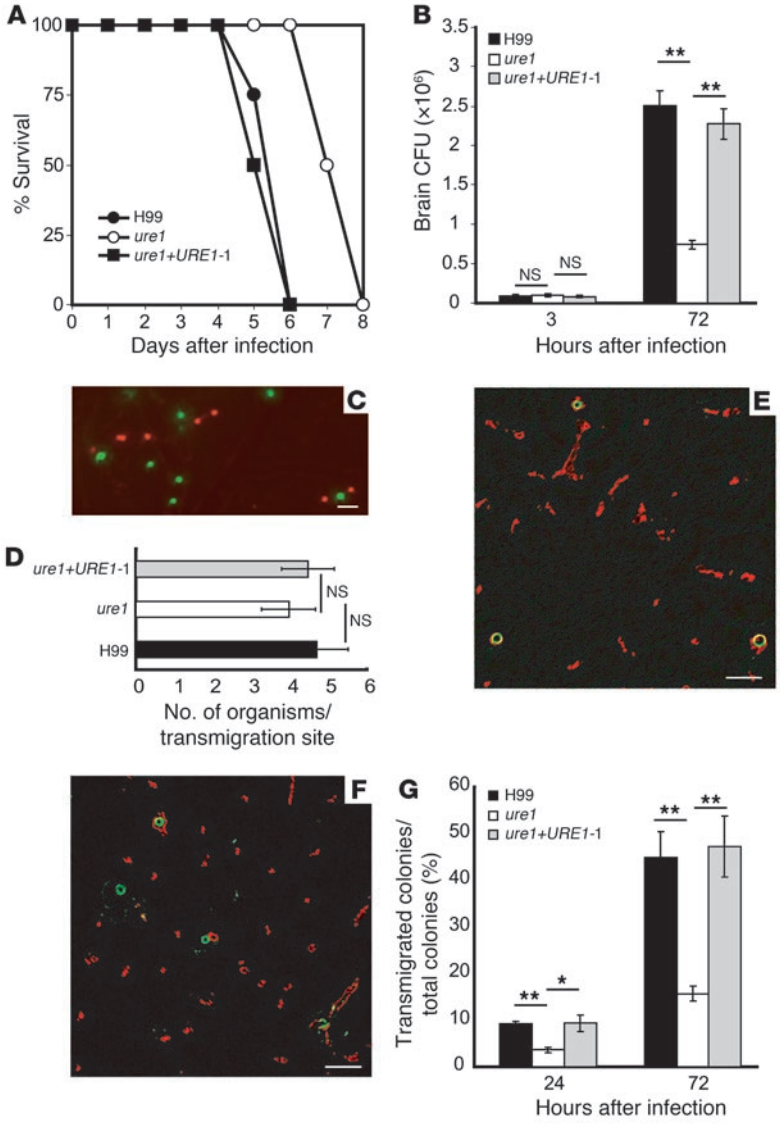

Figure 7
Urease contributes to the transmigration of *C. neoformans* in brain. (**A**) Survival of mice injected i.v. with 20×10^6 *C. neoformans* H99, *ure1*, or *ure1+URE1*-1. (**B**) Brain CFU of mice 3 and 72 hours after i.v. injection of 20×10^6 of *C. neoformans* H99, *ure1*, or *ure1+URE1*-1. (**C**) An image taken by spinning disk confocal microscopy 2 hours after i.v. injection of a mixture of equal numbers (50×10^6) of FITC-labeled *ure1* and TRITC-labeled *ure1+URE1*-1 showing equal distribution of the two yeasts in the capillary bed. (**D**) The number of yeasts at each transmigration site, 72 hours after i.v. injection of 20×10^6 *C. neoformans* H99, *ure1*, or *ure1+URE1*-1. (**E**) An immunofluorescence image from the brain 24 hours after injection of *ure1* showing yeasts (green) located inside vessels (red). (**F**) An immunofluorescence image of the brain taken 24 hours after injection of *ure1+URE1*-1 showing yeasts (green) localized in the parenchyma of the brain as well as inside the vessels (red). (**G**) Percentage of colonies within the parenchyma of the brain (transmigrated) as a percentage of the total colonies, 24 and 72 hours after i.v. injection of 20×10^6 *C. neoformans* H99, *ure1*, or *ure1+URE1*-1. Data are presented as mean ± SEM ($n = 4$). Data are representative of 2 or 3 independent experiments. $^*P < 0.05$, $^{**}P < 0.01$. Scale bars: 20 μm.

ure1+URE1-1 (Figure 7G, $P < 0.05$) at 24 and 72 hours after infection, implicating urease in the process of transmigration.

This raised the possibility that transmigration might be amenable to therapy. For this purpose, we treated the mice and the organisms with flurofamide (EU-4534), a urease inhibitor that has been proposed for clinical use. Survival was prolonged (Figure 8A, $P < 0.05$), significantly lower CFU counts were present in the brain (Figure 8B, $P < 0.05$), and there were significantly fewer transmigration sites (Figure 8C, $P < 0.05$) as compared with control, suggesting that inhibition of urease might be a therapeutic approach to inhibit transmigration of *C. neoformans* across the blood brain barrier.

Discussion

In this study, we demonstrate that (a) *C. neoformans* appears in the brain very quickly after i.v. inoculation and comes to a sudden stop in the capillaries of the brain, with no evidence of a prior reduction in velocity or rolling. (b) The organisms are arrested in vessels of comparable diameter, and neither viability, encapsulation, strain, nor species affected the manner in which *C. neoformans* stopped in the brain vasculature. Moreover, the characteristics were similar to those of an inert particle of the same size. (c) Single organisms, often with a budded morphology, were observed to actively transmigrate across the brain microvasculature. Viability was essential for transmigration, while the ability to proliferate in vivo was not. (d) Urease increases the number of transmigration sites into the brain, resulting in higher CFU counts and reduced survival, which affords a therapeutic opportunity.

The physical-biological interface is a critical component of microbial pathogenesis, virulence, and host defense. Physical factors often control the location, distribution, and movement of microbes within their environment and within the host. For example, acquisition of tuberculosis or some viruses and fungi via the respiratory tract requires exposure to an aerosol containing the microbes. The factors governing exposure and deposition include the density and regional distribution of the particles in the air and the velocity of inspiratory airflow at the time the aerosol is present. Similarly, for blood-borne infections, mechanical forces governing the speed with which the organisms move within the vasculature and regional blood flow may be critical determinants of distribution in the body. Subsequently, microbes pass through an interface

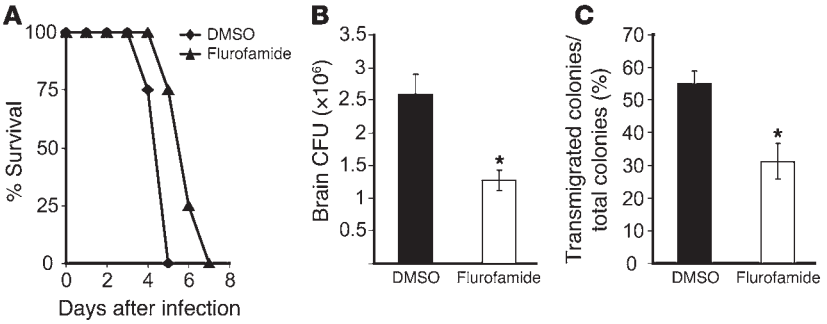

Figure 8

Flurofamide ameliorates brain infection. (**A**) Survival of the mice treated with flurofamide and receiving 20×10^6 flurofamide-treated *C. neoformans* strain H99 compared with DMSO treatment, which served as a control. (**B**) Brain CFU of mice treated with flurofamide and receiving 20×10^6 flurofamide-treated *C. neoformans* strain H99 compared with DMSO treatment. (**C**) Percentage of colonies within the parenchyma of the brain as a percentage of the total colonies at 72 hours in mice treated with flurofamide and receiving 20×10^6 flurofamide-treated *C. neoformans* strain H99. Data are presented as mean ± SEM ($n = 4$). Data are representative of 2 or 3 independent experiments. $^*P < 0.05$.

where biological forces determine their fate. Respiratory viruses make contact with their epithelial receptors and are internalized. *Mycobacterium tuberculosis* is phagocytosed. However, this interface does not necessarily occur when the microbe contacts the host cell. For example, filamentous fungal pathogens use turgor pressure for invasion (24). Thus, the physical-biological interface can actually occur after tissue invasion. Herein, we examine the question of whether the physical-biological interface occurs prior to the arrest of *C. neoformans* in the brain due to fungal receptor–mediated adherence or whether it occurs following arrest, which requires the organism to be trapped. Likewise, the interface could occur following invasion, which would require the physical forces to drive the rigid organism through the endothelial barrier into the tissue or proliferation producing a space-occupying lesion that causes the organisms to burst through the capillary. Understanding the point at which this interface occurs is critical for the development of therapy, since manipulating physical forces requires a very different approach than manipulating biological processes.

Answering these challenging questions has been made possible by advances in imaging techniques. Previous models using histological and electron microscopy approaches have made great contributions to understanding the location of the yeast in the brain microvasculature or cultured endothelial cells during the invasion. However, these techniques are unable to unravel early dynamic events occurring between *C. neoformans* and brain endothelial cells. In this study, a real-time system was developed to directly visualize the early interactions of *C. neoformans* within the brain microvasculature in the living host using IVM.

There are a number of pieces of evidence that the physical-biologic interface occurs after the organism comes to a halt. *C. neoformans* stops on the endothelial surface of the capillary, which is relatively devoid of adhesion molecules compared with the postcapillary venule (28). There is the possibility that stopping might be a consequence of reduced cerebral microcirculation shear. Indeed, it has been recently reported that reduced shear stress in some capillaries (approximately 0.5 dynes/cm^2) compared with the postcapillary venule (3.0 ± 1.5 dynes/cm^2) is associated with *Neisseria meningitidis* attachment in the brain vasculature (29). However, our observations demonstrate that *C. neoformans* did not adhere to cultured endothelial cells under shear stress even when it was as low as 0.03 dyn/cm^2. Thus, it seems unlikely that transient lower shear stress was responsible for the yeast stopping in the capillary. This is supported by the observation that the yeast stopped in capillaries where the size of the vessel was similar to the diameter of the yeast.

Our data clearly demonstrate that viability and capsule do not affect the dynamic process leading to arrest of the yeast. We killed the yeast by heat and studied the effect of capsule, reasoning that they might alter the surface molecular structures and therefore have the potential to affect receptor-ligand interactions. While it is possible that heat-killing the yeast or encapsulation would not alter receptor-ligand interactions, the absence of an effect is most consistent with a mechanical mechanism. Further, while it is obvious that viability and encapsulation are critical determinants of virulence, it is equally clear that they do not play a role during the initial process that brings *C. neoformans* to a halt in the brain.

Strikingly, polystyrene microspheres similar in size to the yeast behave the same as the yeast cells in the brain during the early interaction within the capillary, providing indirect evidence that *C. neoformans* is trapped in the brain capillary by a mechanical mechanism. In keeping with this observation, *C. neoformans* was also trapped in other vascular beds, and other microbes (*S. cerevisiae*) were also trapped. Moreover, the CSP-1 strain of *C. neoformans* displayed the same kinetics of transit and arrest as did the CD44-knockout strain of mice (data not shown). While it is impossible to exclude a contribution by receptor-related interactions, our data provide strong evidence that the mechanism bringing *C. neoformans* to arrest in the brain capillary is the result of mechanical trapping and suggest that particle size is an important determinant of the disease.

The next step was to determine whether the physical-biologic interface occurred beyond the stage leading to penetration of the endothelium. A number of studies have shown that *C. neoformans* gains access to the parenchyma, suggesting that the yeast must cross the brain microvasculature to cause meningoencephalitis. However, the ability of *C. neoformans* to transmigrate into the parenchyma across the brain microvasculature had not previously been shown directly. In this study, we were able to show using immunohistochemistry that the yeast penetrates the capillary wall. We also showed the dynamic process of crossing of the capillary wall by yeast cells in real time using spinning disk confocal IVM. These observations do not invalidate the other "Trojan horse" mechanism by which *Cryptococcus* has also been proposed to cross the brain vasculature, but rather speak only to the direct transit of organisms into the brain (15). Our results further indicate that viability is essential for crossing of brain capillaries by *C. neoformans*, although encapsulation is not. Moreover, polystyrene microspheres were unable to cross the vessels, although they could be trapped in the capillary. Together, these data indicate that a biologic process governs transmigration in that the organisms must be viable. It has been suggested that the organisms might proliferate within the vasculature and via this process rupture the vessel, allowing penetration (15). Indeed, we did find that the organisms must be viable.

However, replication-defective but viable strains were fully capable of penetrating the endothelium and invading the brain.

The observation that *C. neoformans* needed to be viable but not replication-competent to invade the endothelium suggested that a metabolic process was required. Metabolic processes that have been identified in the virulence of *C. neoformans* include laccase (involved in melanin production and required for growth in the brain; refs. 30, 31), enzymes involved in glucuronoxylomannan synthesis (involved in production of polysaccharide capsule; ref. 12), phospholipase B1 (involved in production of eicosanoid metabolites) (32), and urease (15, 27). Undoubtedly, multiple, some as-yet-undiscovered genes, are involved in penetration of the endothelium. However, among this list, urease seemed a likely candidate to influence transmigration. The results show that a urease-deficient strain was less able to transmigrate but had a similar ability to replicate once it had crossed the endothelium. This is consistent with the previous observations by Olszewski et al. (15). There are a number of possible mechanisms by which urease could contribute to transmigration. The enzymatic degradation of urea produces ammonia. Ammonia is highly toxic to brain endothelium as seen in inborn errors of metabolism involving the urea acid cycle and in Reye syndrome, in which there is an accumulation of ammonia (33, 34). Similarly, ammonia produced by urease is toxic to gastric epithelium during *Helicobacter pylori* infection (35). Thus, we might speculate that the local production of ammonia damages the endothelium, increasing permeability and leading to transmigration of *Cryptococcus*. Additionally, it is possible that cryptococcal urease possesses other substrate specificity, which might facilitate transmigration. While these possibilities will require further study, it is notable that urease inhibitors have found application in other areas of medicine. Urease inhibitors such as acetohydroxamic acid are approved for the treatment of nephrolithiasis, where they inhibit bacterial urease and ammonia production. Using one of these inhibitors and exposing the organism to the agent for only 4 hours prior to reaching the brain, we were able to reduce the number of transmigration sites, which translated into a reduced number of CFUs and prolonged survival.

In summary, physical or biologic forces govern exposure, contact, arrest, and invasion of microorganisms. In many cases, physical and mechanical forces govern initial contact and exposure to microbes and may lead to arrest on or in the tissue, and even penetration into the tissue. However, at some point, physical forces must give way to biologic processes for disease to occur. For *C. neoformans*, we provide evidence that mechanical trapping, and therefore size, is a critical determinant and that the interface occurs after arrest, during the process of invasion of the endothelial barrier into the brain, which may be amenable to therapeutic intervention.

Methods

Animals. Female 8- to 10-week-old C57BL/6 mice were purchased from Charles River Laboratories. Female, 8- to 10-week-old Tie-2 GFP BALB/c mice were purchased from The Jackson Laboratory. The mice were kept in polycarbonate cages on sawdust and allowed free access to food and water throughout the experiments. All animal studies were approved by the IACUC of the University of Calgary (protocol m08005) according to the recommendations of the Canadian Council of Animal Care.

C. neoformans. Strain H99 encapsulated, serotype A (catalog 208821), B3501 (catalog 34873), and CAP67, an acapsular mutant of B3501 (catalog 52817), were obtained from the ATCC. The temperature-sensitive strains *ras1* mutant, *ras1+RAS1* reconstituted, *cdc24* mutant, and *cdc24+CDC24* reconstituted in H99 background were obtained from J. Andrew Alspaugh, Duke University Medical Center, Durham, North Carolina, USA (25, 26). The urease-knockout strain *ure1* (urease-negative transformant of H99 with a selective disruption of native urease gene, *URE1*) and the urease-restored strain *ure1+URE1*-1 (strain *ure1* rescued with a wild-type copy of the *URE1* gene) were a generous gift of Gary Cox (Duke University) (27) and obtained from Michal A. Olszewski, University of Michigan Medical Center, Ann Arbor, Michigan, USA (15). The organisms were grown on Sabouraud's dextrose agar (Difco) and maintained on slants, passaged each month as described previously (36). *C. neoformans* was grown to log phase in Sabouraud's dextrose broth (Difco) at 32°C with gentle rotation for 24 hours and then washed 3 times in sterile PBS (pH 7.4). In some experiments, fungus was heat-killed at 50°C overnight (37) before use. The live or heat-killed organisms were labeled with FITC (Sigma-Aldrich) or TRITC (Sigma-Aldrich) as described previously (38, 39). In brief, the organisms were suspended at 2×10^8/ml in FITC or TRITC at 500 μg/ml in PBS, incubated for 10 minutes at 37°C, and extensively washed in PBS.

Flow chamber assay. A flow chamber assay using primary HUVECs and an HBMEC line was performed as described previously (17, 18). In brief, human umbilical cord veins (Foothills Hospital, Calgary, Alberta, Canada) were rinsed of blood products with warm PBS, pH 7.4, and the vein was filled with warm collagenase A (Roche Diagnostics; used at a concentration of 320 U/ml in PBS). After 20 minutes of incubation in warm PBS, the digest was collected into centrifuge tubes containing heat-inactivated FBS (Hyclone) to neutralize the collagenase activity. The cells were centrifuged, the supernatant discarded, and the cells were seeded and cultured on glass coverslips in M199 media with 20% human serum. The cells were cultured into a monolayer within 1 week. HUVECs forming a confluent monolayer on a coverslip were placed in the flow chamber. HUVECs on glass coverslips were either treated with 10 ng/ml LPS (*Escherichia coli* serotype O111:B4; Calbiochem) for 4 hours or left untreated. The HBMEC line (40, 41) was thawed and cultured in a monolayer on a coverslip in RPMI 1640 medium supplemented with 10% (vol/vol) FBS, 10% NuSerum, L-glutamine (2 mM), sodium pyruvate (1 mM), 1% MEM nonessential amino acids (all from Invitrogen Life Technologies), 1% vitamins (Sigma-Aldrich), 100 U/ml penicillin, and 100 μg/ml streptomycin (Invitrogen). HBMECs forming a confluent monolayer on a coverslip were placed in the flow chamber.

The flow chamber was placed on an inverted microscope stage, which was enclosed with a warm air cabinet, and the temperature was maintained at 37°C. A syringe pump (Harvard Apparatus) was used to draw *C. neoformans* (strain H99) derived from in vitro culture or freshly donated heparinized blood (as positive control) from a healthy donor over monolayers at a shear of 2, 1, 0.5, 0.25, 0.13, 0.06, or 0.03 dyn/cm^2. Interactions of *C. neoformans* or leukocytes (as positive controls) with HUVECs or HBMECs were visualized by phase contrast microscopy and recorded via a CCD camera (KP-M1U; Hitachi Denshi Ltd.) for later analysis.

IVM. IVM of the brain microcirculation was performed as previously described (20, 42, 43). Briefly, C57BL/6 mice were anesthetized by i.p. injection of a mixture of 10 mg/kg xylazine (MTC Pharmaceuticals) and 200 mg/kg ketamine hydrochloride (Rogar/STB). The body temperature of mice was kept at 36–37°C throughout the experiment. A craniotomy was performed using a high-speed drill (Fine Science Tools), and the durometer was gently removed to expose the underlying pial vasculature. The exposed brain was kept moist with an artificial cerebrospinal fluid throughout the experiment.

The mice were inoculated i.v. by the tail vein with fluorescently labeled *C. neoformans* or fluorescent polystyrene microspheres of a size similar to that of *C. neoformans* (5.68 ± 0.43 μm; Polysciences Inc.) or FITC-labeled *S. cerevisiae* (Fleischmann's Traditional Yeast). In vivo yeast cell and endothelial cell interactions were observed using a microscope (Zeiss Axioskop) outfitted with a fluorescent light source. A low light intensified

CCD camera (Stanford Photonics) mounted on the microscope was used to project the image to a monitor. All experiments were recorded for later playback and analysis. The number of yeast cells and polystyrene microspheres passing through postcapillary venules (with a diameter between 30 and 70 μm) at various time points after injection, as well as the number and time of the yeast cells and polystyrene microspheres arresting in the capillary bed, were determined off-line during video playback analysis.

Spinning disk confocal IVM. The brain microcirculation of C57BL/6 mice was prepared for spinning disk confocal IVM as described above. Images were acquired with an Olympus B×51 upright microscope (44). The microscope was equipped with a confocal light path (WaveFx, Quorum) based on a modified Yokogawa CSU-10 head (Yokogawa Electric Corp.). In some experiments, Tie-2 GFP BALB/c mice were injected i.v. with 100×10^6 TRITC-labeled (Sigma-Aldrich) *C. neoformans* (strain H99). In other experiments, C57BL/6 mice were injected with a mixture of equal numbers of encapsulated H99 and B3501, or B3501 and acapsular Cap67, H99 and heat-killed H99, or *ure1* and *ure1+URE1*-1 following labeling with FITC or TRITC, respectively. Disruption and reconstitution of urease by these strains was confirmed by using the CLOtest Rapid Urease Test (Kimberly-Clark/Ballard Medical Products). Laser excitation wavelengths of both 488 and 561 nm were used in rapid succession and visualized with the appropriate long-pass filters (Semrock). Typical exposure time for both excitation wavelengths was 168 ms. A 512 × 512–pixel back-thinned electron-multiplying charge-coupled device camera (C9100-13, Hamamatsu) was used for fluorescence detection. Volocity Acquisition software (Improvision) was used to drive the confocal microscope.

Immunohistochemistry. Following i.v. injection, mice were sacrificed, and the brain was removed for immunohistochemical staining to visualize the yeast cells. To avoid contamination of tissues by circulating fungus, perfusion was performed by injecting sterile saline (50 ml) into the left ventricle, the right atrium being cut open to allow drainage during the procedure (12). The brain tissues of mice injected with unlabeled yeast cells were prepared for paraffin sectioning as described previously (12, 45). In brief, the tissues were fixed in 10% neutral buffered formalin for 24 hours at 4°C, embedded in paraffin, and cut into 5-μm sections. The tissues were deparaffinized in xylene and rehydrated through a graded series of ethanol. The tissues were treated with EDTA (10 mM, pH 8.0) for 40 minutes in a rice steamer, followed by blocking with 2% goat serum in PBS. Sections were then incubated with a mouse mAb specific for cryptococcal polysaccharide (E1, a gift from Françoise Dromer, Institut Pasteur, Paris, France; ref. 46) or 18B7 (a gift from Arturo Casadevall, Albert Einstein College of Medicine, New York, New York, USA; ref. 47), and a rabbit anti-collagen IV Ab (Chemicon) that delineated brain capillaries by staining the basal lamina (12) at 4°C overnight. After 3 washes, sections were incubated for 30 minutes with Alexa Fluor 488 goat anti-rabbit IgG (H+L) and Alex Fluor 555 goat anti-mouse IgG (H+L) (Invitrogen). Alternatively, sections were incubated for 30 minutes with Alex Fluor 555 goat anti-rabbit IgG (H+L) and Alex Fluor 488 goat anti-mouse IgG (H+L) (Invitrogen). The brain tissues of mice injected with FITC-labeled yeast cells or fluorescence-labeled polystyrene microspheres were prepared for frozen sections as described previously (48). In brief, the tissues were removed and frozen in OCT compound. Frozen tissue blocks were cut on a cryostat microtome, and 6- to 7-μm sections were placed on coated glass slides. Tissue sections were fixed in 2% neutral buffered paraformaldehyde for 10 minutes. Sections were then incubated with 2% goat serum in PBS, followed by incubation with an anti–collagen IV Ab at 4°C overnight. After 3 washes, sections were incubated for 30 minutes with Alex Fluor 555 goat anti-rabbit IgG (H+L) or Alexa Fluor 488 goat anti-rabbit IgG (H+L) (Invitrogen) to delineate brain microvasculature. The sections were rinsed and mounted with glycerol. Immunofluorescence images of tissue sections were obtained at ×20, ×40, or ×100 objective magnification using an Olympus I×70 microscope equipped with digital deconvolution (DeltaVision; Applied Precision). The *z*-sections of fluorescence images were recorded at successive 0.2-μm intervals through the entire thickness of the sections. Each image shown in this article consists of a single *z*-section.

Survival and brain CFU. C57BL/6 mice were injected with 20×10^6 H99, *ure1*, or *ure1+URE1*-1 by tail vein. In some experiments, groups of mice were i.p. injected with 1.5 mg (per mouse) of the urease inhibitor flurofamide (Tocris Bioscience) dissolved in DMSO, or DMSO alone as control. Four hours later, the mice treated with flurofamide were injected i.v. with H99 pretreated with 7.5 mM flurofamide diluted with 15% DMSO for 4 hours at room temperature. As a control, the mice treated with DMSO alone were injected i.v. with H99 pretreated with 15% DMSO for 4 hours at room temperature. Twenty-four hours later, the mice were injected i.p. with 0.75 mg flurofamide dissolved in DMSO or DMSO alone (control). The survival of the mice was observed every 4 hours. To determine the burden of organisms, the mice were killed at various times after infection. Brains were dissected and homogenized in sterile water. Appropriate dilutions of the homogenates were plated onto Sabouraud's dextrose agar plates, and CFU were enumerated after 24–48 hours growth at 30°C. To assess the transmigration and growth of the yeast, the brain was removed and immunohistochemistry performed to label the yeast and vessels as described above. Each cluster of organisms was considered to be one colony. If the colony was outside the vessel, it was considered to be a transmigration site. The colonies both inside and outside the vessels in the brain were enumerated. The number of the yeast cells in each colony was determined. The activity of flurofamide was confirmed by attenuation of color development using the CLOtest Rapid Urease Test (Kimberly-Clark/Ballard Medical Products). For this purpose, The H99 strain (100×10^6/ml) was added to 15% DMSO or 7.5 mM flurofamide diluted with 15% DMSO for 60 minutes at room temperature. Five microliters of the suspension was added into the CLOtest detection kit, and the color change was observed 2 hours later.

Statistics. Data were expressed as mean ± SEM. An ANOVA was performed to establish equal variance, and 2-tailed Student's *t* test with Bonferroni correction was applied to determine statistical significance, which was defined as $P < 0.05$.

Acknowledgments

We would like to thank Brandie Millen, Pina Colarusso, Lita McDonald, Chris Meijndert, and the Canadian Institutes of Health Research group grant–funded microscopy core facility for training and assistance related to microscopy and image acquisition. We are also grateful to Brandie Millen, Caroline Leger, and Carol Gwozd for technical support. This work was funded by a grant from the Lung Association of Alberta and the North West Territories to C.H. Mody and M. Shi; and an equipment and infrastructure grant from the Canadian Foundation for Innovation (CFI) and the Alberta Science and Research Authority.

Received for publication December 8, 2009, and accepted in revised form March 3, 2010.

Address correspondence to: Christopher H. Mody, Department of Internal Medicine and Microbiology and Infectious Diseases, Snyder Institute for Infection, Inflammation and Immunity, Rm. 4AA14 Health Research Innovation Centre (HRIC), University of Calgary, Calgary, Alberta, Canada T2N 4N1. Phone: 403.220.8479; Fax: 403.210.8463; E-mail: cmody@ucalgary.ca.

1. Kim KS. Pathogenesis of bacterial meningitis: from bacteraemia to neuronal injury. *Nat Rev Neurosci*. 2003;4(5):376–385.
2. Lee SC, Dickson DW, Casadevall A. Pathology of cryptococcal meningoencephalitis: analysis of 27 patients with pathogenetic implications. *Hum Pathol*. 1996;27(8):839–847.
3. Mitchell TG, Perfect JR. Cryptococcosis in the era of AIDS--100 years after the discovery of *Cryptococcus neoformans*. *Clin Microbiol Rev*. 1995;8(4):515–548.
4. Gottfredsson M, Perfect JR. Fungal meningitis. *Semin Neurol*. 2000;20(3):307–322.
5. Kwon-Chung KJ, Sorrell TC, Dromer F, Fung E, Levitz SM. Cryptococcosis: clinical and biological aspects. *Med Mycol*. 2000;38(suppl 1):205–213.
6. Chretien F, Lortholary O, Kansau I, Neuville S, Gray F, Dromer F. Pathogenesis of cerebral *Cryptococcus neoformans* infection after fungemia. *J Infect Dis*. 2002;186(4):522–530.
7. Johnston B, Walter UM, Issekutz AC, Issekutz TB, Anderson DC, Kubes P. Differential roles of selectins and the alpha4-integrin in acute, subacute, and chronic leukocyte recruitment in vivo. *J Immunol*. 1997;159(9):4514–4523.
8. Norman MU, Moriarty TJ, Dresser AR, Millen B, Kubes P, Chaconas G. Molecular mechanisms involved in vascular interactions of the Lyme disease pathogen in a living host. *PLoS Pathog*. 2008; 4(10):e1000169.
9. Prasadarao NV, Wass CA, Huang SH, Kim KS. Identification and characterization of a novel Ibe10 binding protein that contributes to *Escherichia coli* invasion of brain microvascular endothelial cells. *Infect Immun*. 1999;67(3):1131–1138.
10. Ring A, Weiser JN, Tuomanen EI. Pneumococcal trafficking across the blood-brain barrier. Molecular analysis of a novel bidirectional pathway. *J Clin Invest*. 1998;102(2):347–360.
11. Chang YC, et al. Cryptococcal yeast cells invade the central nervous system via transcellular penetration of the blood-brain barrier. *Infect Immun*. 2004;72(9):4985–4995.
12. Charlier C, Chretien F, Baudrimont M, Mordelet E, Lortholary O, Dromer F. Capsule structure changes associated with *Cryptococcus neoformans* crossing of the blood-brain barrier. *Am J Pathol*. 2005; 166(2):421–432.
13. Chen SH, et al. *Cryptococcus neoformans* induces alterations in the cytoskeleton of human brain microvascular endothelial cells. *J Med Microbiol*. 2003; 52(pt 11):961–970.
14. Ibrahim AS, Filler SG, Alcouloumre MS, Kozel TR, Edwards JE Jr, Ghannoum MA. Adherence to and damage of endothelial cells by *Cryptococcus neoformans* in vitro: role of the capsule. *Infect Immun*. 1995;63(11):4368–4374.
15. Olszewski MA, et al. Urease expression by *Cryptococcus neoformans* promotes microvascular sequestration, thereby enhancing central nervous system invasion. *Am J Pathol*. 2004;164(5):1761–1771.
16. Santangelo R, et al. Role of extracellular phospholipases and mononuclear phagocytes in dissemination of cryptococcosis in a murine model. *Infect Immun*. 2004;72(4):2229–2239.
17. Lloyd KL, Kubes P. GPI-linked endothelial CD14 contributes to the detection of LPS. *Am J Physiol Heart Circ Physiol*. 2006;291(1):H473–481.
18. Ostrovsky L, Carvalho-Tavares J, Woodman RC, Kubes P. Translational inhibition of E-selectin expression stimulates P-selectin-dependent neutrophil recruitment. *Am J Physiol Heart Circ Physiol*. 2000; 278(4):H1225–H1232.
19. Nimmerjahn A, Kirchhoff F, Helmchen F. Resting microglial cells are highly dynamic surveillants of brain parenchyma in vivo. *Science*. 2005; 308(5726):1314–1318.
20. Zhou H, Lapointe BM, Clark SR, Zbytnuik L, Kubes P. A requirement for microglial TLR4 in leukocyte recruitment into brain in response to lipopolysaccharide. *J Immunol*. 2006;177(11):8103–8110.
21. Albelda SM, Smith CW, Ward PA. Adhesion molecules and inflammatory injury. *FASEB J*. 1994;8(8):504–512.
22. Zarbock A, Ley K. Neutrophil adhesion and activation under flow. *Microcirculation*. 2009;16(1):31–42.
23. Steenbergen JN, Casadevall A. Prevalence of *Cryptococcus neoformans var. neoformans* (Serotype D) and *Cryptococcus neoformans var. grubii* (Serotype A) isolates in New York City. *J Clin Microbiol*. 2000; 38(5):1974–1976.
24. Bastmeyer M, Deising HB, Bechinger C. Force exertion in fungal infection. *Annu Rev Biophys Biomol Struct*. 2002;31:321–341.
25. Alspaugh JA, Cavallo LM, Perfect JR, Heitman J. RAS1 regulates filamentation, mating and growth at high temperature of *Cryptococcus neoformans*. *Mol Microbiol*. 2000;36(2):352–365.
26. Nichols CB, Perfect ZH, Alspaugh JA. A Ras1-Cdc24 signal transduction pathway mediates thermotolerance in the fungal pathogen *Cryptococcus neoformans*. *Mol Microbiol*. 2007;63(4):1118–1130.
27. Cox GM, Mukherjee J, Cole GT, Casadevall A, Perfect JR. Urease as a virulence factor in experimental cryptococcosis. *Infect Immun*. 2000;68(2):443–448.
28. Coisne C, et al. Differential expression of selectins by mouse brain capillary endothelial cells in vitro in response to distinct inflammatory stimuli. *Neurosci Lett*. 2006;392(3):216–220.
29. Mairey E, et al. Cerebral microcirculation shear stress levels determine *Neisseria meningitidis* attachment sites along the blood-brain barrier. *J Exp Med*. 2006;203(8):1939–1950.
30. Barluzzi R, et al. Establishment of protective immunity against cerebral cryptococcosis by means of an avirulent, non melanogenic *Cryptococcus neoformans* strain. *J Neuroimmunol*. 2000;109(2):75–86.
31. Salas SD, Bennett JE, Kwon-Chung KJ, Perfect JR, Williamson PR. Effect of the laccase gene CNLAC1, on virulence of *Cryptococcus neoformans*. *J Exp Med*. 1996;184(2):377–386.
32. Noverr MC, Cox GM, Perfect JR, Huffnagle GB. Role of PLB1 in pulmonary inflammation and cryptococcal eicosanoid production. *Infect Immun*. 2003; 71(3):1538–1547.
33. McClung HJ, et al. Early changes in the permeability of the blood-brain barrier produced by toxins associated with liver failure. *Pediatr Res*. 1990; 28(3):227–231.
34. Ziylan YZ, Uzum G, Bernard G, Diler AS, Bourre JM. Changes in the permeability of the blood-brain barrier in acute hyperammonemia. Effect of dexamethasone. *Mol Chem Neuropathol*. 1993;20(3):203–218.
35. Smoot DT, Mobley HL, Chippendale GR, Lewison JF, Resau JH. *Helicobacter pylori* urease activity is toxic to human gastric epithelial cells. *Infect Immun*. 1990;58(6):1992–1994.
36. Mody CH, Toews GB, Lipscomb MF. Cyclosporin A inhibits the growth of *Cryptococcus neoformans* in a murine model. *Infect Immun*. 1988;56(1):7–12.
37. Martinez LR, Garcia-Rivera J, Casadevall A. *Cryptococcus neoformans var. neoformans* (serotype D) strains are more susceptible to heat than *C. neoformans var. grubii* (serotype A) strains. *J Clin Microbiol*. 2001;39(9):3365–3367.
38. Walenkamp AM, Scharringa J, Schramel FM, Coenjaerts FE, Hoepelman IM. Quantitative analysis of phagocytosis of *Cryptococcus neoformans* by adherent phagocytic cells by fluorescence multi-well plate reader. *J Microbiol Methods*. 2000;40(1):39–45.
39. Alvarez M, Casadevall A. Phagosome extrusion and host-cell survival after *Cryptococcus neoformans* phagocytosis by macrophages. *Curr Biol*. 2006; 16(21):2161–2165.
40. Stins MF, Badger J, Sik Kim K. Bacterial invasion and transcytosis in transfected human brain microvascular endothelial cells. *Microb Pathog*. 2001; 30(1):19–28.
41. Stins MF, Nemani PV, Wass C, Kim KS. *Escherichia coli* binding to and invasion of brain microvascular endothelial cells derived from humans and rats of different ages. *Infect Immun*. 1999;67(10):5522–5525.
42. Kerfoot SM, Kubes P. Overlapping roles of P-selectin and alpha 4 integrin to recruit leukocytes to the central nervous system in experimental autoimmune encephalomyelitis. *J Immunol*. 2002; 169(2):1000–1006.
43. Lapointe BM, Herx LM, Gill V, Metz LM, Kubes P. IVIg therapy in brain inflammation: etiology-dependent differential effects on leucocyte recruitment. *Brain*. 2004;127(pt 12):2649–2656.
44. Norman MU, Hulliger S, Colarusso P, Kubes P. Multichannel fluorescence spinning disk microscopy reveals early endogenous CD4 T cell recruitment in contact sensitivity via complement. *J Immunol*. 2008;180(1):510–521.
45. Shi M, Pan W, Tabel H. Experimental African trypanosomiasis: IFN-gamma mediates early mortality. *Eur J Immunol*. 2003;33(1):108–118.
46. Dromer F, Salamero J, Contrepois A, Carbon C, Yeni P. Production, characterization, and antibody specificity of a mouse monoclonal antibody reactive with *Cryptococcus neoformans* capsular polysaccharide. *Infect Immun*. 1987;55(3):742–748.
47. Lendvai N, Casadevall A. Monoclonal antibody-mediated toxicity in *Cryptococcus neoformans* infection: mechanism and relationship to antibody isotype. *J Infect Dis*. 1999;180(3):791–801.
48. Shi M, Huther S, Burkhardt E, Zahner H. Lymphocyte subpopulations in the caecum mucosa of rats after infections with *Eimeria separata*: early responses in naive and immune animals to primary and challenge infections. *Int J Parasitol*. 2001;31(1):49–55.